## IV.1 Estudio de los sistemas mixtos de NiO-MgO.

De los antecedentes bibliográficos sobre la hidrogenación de dinitrilos en fase gas se concluye que la selectividad en esta reacción está relacionada con la estructura de la fase activa y con la basicidad. Así, es posible obtener selectivamente compuestos monohidrogenados a partir de dinitrilos y más concretamente 6-aminohexanonitrilo a partir de 1,6-hexanodinitrilo (adiponitrilo).

Sobre la base de estas consideraciones se han diseñado unas metodologías preparativas que nos conduzcan a sistemas catalíticos con estructuras bien definidas y una basicidad adecuada.

### IV.1.1 Requisitos de los sistemas catalíticos.

*1.- Control estructural.*

La morfología octaédrica de las partículas de óxido de níquel conduce, después de su reducción, a la obtención tener catalizadores de Ni que inducen, según trabajos anteriores, selectividad hacia compuestos monohidrogenados [18]. Este hecho indica que es posible entender la reacción catalítica del adiponitrilo como una reacción sensible a la estructura y que hay diferentes requisitos estructurales para los centros activos, que son los responsables de la obtención del compuesto 6-aminohexanonitrilo de forma selectiva. Sin embargo, problemas como la sinterización en la etapa de reducción y la interacción entre la fase activa y el soporte pueden ser claves en la definición de la morfología octaédrica y por tanto en su selectividad.

Respecto a la obtención de morfología octaédrica, varios estudios han mostrado que mediante la descomposición directa de nitrato de níquel hexahidrato se obtiene un óxido de níquel no-estequiométrico, poco homogéneo formado por partículas con una cierta morfología octaédrica de tamaños muy diferentes [18, 69].

La optimización del proceso de obtención se realizó mediante diferentes estudios de descomposición controlada buscando obtener un precursor más homogéneo y mantener la morfología octaédrica [69]. De estos estudios se concluyó que la termólisis controlada del nitrato de níquel hexahidrato hasta la obtención de la especie básica $Ni_3(NO_3)_2(OH)_4$ generaba posteriormente en el proceso de calcinación, la formación de un óxido de níquel no-estequiométrico de morfología octaédrica y con tamaños de partícula homogéneos.

*2.- Basicidad.*

Un cierto carácter básico en los sistemas catalíticos parece favorecer la eliminación de aminas y disminuir las reacciones secundarias de condensación, las cuales son posiblemente la principal causa de envenenamiento del catalizador, con lo que sería posible alargar la vida activa de los catalizadores. No obstante, un exceso de basicidad favorece la ciclación de Thorpe, que es la ciclación intramolecular del propio dinitrilo, producto difícilmente eliminable y que conduce también a la desactivación del catalizador [20].

Las magnesias son materiales de basicidad moderada, y al igual que la mayoría de materiales pueden presentar diferentes características según el procedimiento de obtención utilizado. Así, se puede disponer de magnesias con áreas desde unos pocos metros cuadrados a valores superiores a 200 $m^2g^{-1}$. No obstante, todas las

magnesias tienen en común su alta sensibilidad al agua, de forma que pequeñas cantidades de ésta pueden conducir a una alta aglomeración.

### IV.1.2 Diseño de precursores y catalizadores.

La preparación de los diferentes precursores NiO-MgO y los estudios realizados de los mismos se han desarrollado en dos partes.

*1.- Estudio de las condiciones de preparación de los sistemas NiO-MgO con en el fin de controlar la homogeneidad de la morfología y el tamaño de partícula de la fase óxido de níquel.*

- En este trabajo se ha buscado en primer lugar obtener la fase $Ni_3(NO_3)_2(OH)_4$ en presencia de magnesia, realizando un estudio de descomposición de nitrato de níquel hexahidrato a diferentes temperaturas y siguiendo la evolución de las diferentes fases mediante difracción de rayos X.

- Se han utilizado tres magnesias de diversas procedencias y con diferentes áreas superficiales (magnesias C1, N, A). También se han variado las cantidades iniciales de $Ni(NO_3)_2.6H_2O$/MgO para obtener diferentes proporciones másicas NiO/MgO (relaciones 1 y 4).

- Los sistemas de NiO-MgO se han preparado mediante dos vías diferentes, obteniéndose soluciones sólidas entre las fases.

A) Mezcla homogénea de óxido de magnesio con el nitrato de níquel hexahidrato y posterior calcinación, vía A.

B) Mezcla homogénea de óxido de magnesio con nitrato de níquel hexahidrato, descomposición térmica a temperatura controlada para la obtención de la especie $Ni_3(NO_3)_4(OH)_4$ y posterior calcinación, vía B.

- Por último se ha realizado un estudio exhaustivo de la reducibilidad de los diferentes sistemas NiO-MgO.

*2.- Diseño de diferentes vías preparativas para obtener sistemas NiO-MgO que se ajusten a las características estructurales buscadas.*

- Utilizando la misma magnesia comercial $C_2$ y dos proporciones 1 y 4 de NiO/MgO, se han probado diversas vías preparativas con el fin de obtener sistemas mixtos con diferentes características superficiales mediante la modificación de la interacción entre la fase NiO y MgO.

Así se han desarrollado diferentes vías para obtener sistemas que presenten solución sólida (A y B) y otras vías en las cuales se obtengan las fases separadas (C y D).

- Se ha realizado un estudio de los diferentes sistemas preparados mediante la vía C, relacionando el área superficial generada con el tiempo y la temperatura de calcinación en flujo de argón.

- Se han estudiado las diferentes reducibilidades de los sistemas preparados mediante las diferentes vías y con las diferentes proporciones másicas NiO/MgO.

**IV.1.3 Estudio de las condiciones de preparación de los sistemas NiO-MgO para controlar sus propiedades.**

*Solid State Ionics, Vol. 134 (3-4) páginas 229-239*

*PII: S0167-2738(00)00772-4*


Study of preparation conditions of NiO-MgO systems to control the morphology and particle size of the NiO phase.

Marc Serra[a], Pilar Salagre[a*], Yolanda Cesteros[a], Francisco Medina[b] and Jesús E. Sueiras[b].

*[a] Facultat de Química, Universitat Rovira i Virgili, Pl. Imperial Tarraco,1. 43005, Tarragona, Spain. e-mail:salagre@quimica.urv.es*

*[b] Escola Tècnica Superior d'Enginyeria Química, Universitat Rovira i Virgili,*

*Pl. Imperial Tarraco,1. 43005, Tarragona, Spain*

**ABSTRACT**

Several NiO-MgO samples were prepared from nickel nitrate hexahydrate and different sources of magnesia by using a NiO/MgO weight ratio of 1:1 and 4:1 and two different preparative paths. All the samples were structurally characterized using BET, XRD, SEM and TPR techniques. The results showed that the sequence of decomposition of the $Ni(NO_3)_2 \cdot 6H_2O$-MgO systems is similar to the sequence reported for the nickel nitrate hexahydrate without magnesia. XRD identified complete solid solutions for all the NiO-MgO systems prepared. Their BET areas were similar but their different morphologies and particles sizes mainly depended on the preparative path. Independently of the magnesia used, the NiO-MgO systems prepared by controlled decomposition of the nickel nitrate hexahydrate until $Ni_3(NO_3)_2(OH)_4$ was formed and which were subsequently calcined to form NiO (path B) led to very homogenous particles of sizes around 100 nm. Path B also gave the highest degrees of NiO reduction.

*Key Words:* nickel nitrate hexahydrate; magnesium oxide; controlled thermal analysis; solid solution; nickel oxide reducibility.

**INTRODUCTION**

The properties of nickel and magnesium oxides and their applicability as catalysts have been widely studied [1-3]. In its reduced form, nickel oxide has been mainly used for such reactions as the hydrogenation of nitriles [4-6] and the hydrodechlorination of aromatic compounds [7-8]. On the other hand, the magnesium oxide has been directly used as catalytic support [9-10] and as basic catalyst [11] in such reactions as aldolic condensation, isomerization of double bonds [10], methane steam reforming [12], methane partial oxidation [13] and oxidative methylation of acetonitrile [14]. Additionally, NiO/MgO catalytic systems, with magnesium in the oxide phase and nickel in the metallic phase, have proved to have a considerable inhibitory effect on the generation of graphitic residuals which substantially deactivate the catalysts [15].

The key factor in obtaining oxides with different properties has been the use of different preparative methods. In the literature, we have found nickel and magnesium oxides which have been prepared with different degrees of crystallinity, particle sizes which vary from nanophases to millimeters [16], morphological differences and BET areas range from values as low as 1 $m^2g^{-1}$ to values as high as 150 $m^2g^{-1}$ [17-18].

The decomposition of nickel nitrate hexahydrate is a procedure which has been described and widely studied [18-20], and which can be performed in controlled conditions of water pressure to obtain the nickel nitrate anhydrous as the direct precursor of NiO. The NiO obtained by this method has a much higher area (about 50 $m^2g^{-1}$) than the NiO formed by decomposition in stationary air (about 1 $m^2g^{-1}$) using a basic nitrate as precursor [21].

In previous studies, we observed that the samples prepared by controlled decomposition have both homogenous morphologies and particle sizes [18].

A high-area (> 200 $m^2g^{-1}$) magnesia can be prepared by calcining magnesium hydroxide under vacuum. When these precursors are calcined in air, the area of the MgO obtained is often low. This is mainly due to the sintering phenomena that takes place in the presence of water vapour [10].

The high susceptibility of magnesia to sintering should be taken into account for subsequent uses. Incorporating divalent cations (Ni, Cu and Zn), preferably during the development of the surface area, is a good means of stabilizing the area of the magnesias prepared [10].

A considerable number of works from the 70's have been focused on the study of the physical and chemical properties of the NiO-MgO system. On the whole, it is accepted that the reactivity is highly affected by the tendency to form solid solutions [22]. Parmaliana et al. [22-24] reported the influence of the calcination temperature and the % nickel weight on the structure and morphology of the mixed systems. They also pointed out that the formation of solid solutions decreases the reducibility of the NiO phase.

The aim of this work is to study the key factors which affect the structural and surface properties as well as the reducibility of the NiO-MgO systems. Samples were characterized by different techniques. We discuss here how affect the use of magnesia obtained from several sources, the different procedures used to decompose the nickel nitrate hexahydrate to NiO and the range in the NiO/MgO weight ratio.

## EXPERIMENTAL

### Sample preparation

#### *MgO preparation*

The magnesium oxides used were obtained in three different ways:

a) MgO commercial referred to as $MgO_{C1}$.

b) MgO prepared by the thermal decomposition of magnesium nitrate hexahydrate at 773 K for 4 hours, referred to as $MgO_N$.

c) MgO prepared by the thermal decomposition of magnesium acetate tetrahydrate at 673 K for 2 hours, referred to as $MgO_A$.

#### *NiO-MgO preparation*

Seven NiO-MgO samples were prepared by modifying different factors: the weight ratio of NiO/MgO, the MgO source and/or the preparative procedure.

The NiO/MgO ratios used were 1:1 and 4:1 (referred to as 1 and 4, respectively). The MgO sources used were three: $MgO_{C1}$, $MgO_N$ and $MgO_A$ (referred to as $C_1$, N and A, respectively) and were obtained as mentioned above. Two preparative procedures were used: path A and path B (referred to as A and B, respectively).

Path A) First, a homogeneous physical mixture of $Ni(NO_3)_2{\cdot}6H_2O$ and MgO was prepared. Then, the samples were calcined at 673 K for 4 hours. These samples are referred to as $1C_1A$, 1NA, $4C_1A$ and 4NA.

Path B) In this procedure, a homogeneous physical mixture of $Ni(NO_3)_2{\cdot}6H_2O$ and MgO was prepared. Then, a controlled thermolysis

study of the nickel nitrate at different temperatures (373 K, 403 K and 433 K) was performed in order to obtain $Ni_3(NO_3)_2(OH)_4$ as a single phase. The samples prepared by thermolysis at 433 K for 7 days are referred to as $P4C_1B$, P4NB and P4AB. These precursors were later calcined at 523 K for 4 hours (samples $4C_1B$, 4NB and 4AB).

**X-ray diffaction (XRD)**

Powder X-ray diffraction patterns of the different samples were obtained with a Siemens D5000 diffractometer using nickel-filtered Cu Kα radiation. Samples were dusted on double-sided sticky tape and mounted on glass microscope slides. The patterns were recorded over a range of 2θ angles from 10º to 90º and crystalline phases were identified using the Joint Committee on Powder Diffraction Standards (JCPDS) files.

The XRD patterns of MgO are very similar to those of NiO. The peak positions corresponding to 2θ angles (with the relative intensities in parentheses), taken from the JCPDS files, are: 36.95 (10), 42.91 (100), 62.31 (52), 74.68 (4) and 78.61 (12) for the MgO phase and 37.28 (91), 43.30 (100), 62.92 (57), 75.44 (16) and 79.39 (13) for the NiO phase. Both 2θ peaks are assigned to the faces (1 1 1), (2 0 0), (2 2 0), (3 1 1) and (2 2 2), respectively.

**BET areas**

BET areas were calculated from the nitrogen adsorption isotherms at 77 K using a Micromeritics ASAP 2000 surface analyser and a value of 0.164 $nm^2$ for the cross-section of the nitrogen molecule.

**Temperature-programmed reduction (TPR)**

Temperature-programmed reductions (TPR) were carried out in a Labsys/Setaram TG DTA/DSC thermobalance equipped with a 273-1273 K progammable temperature furnace. The accuracy was ±1μg.

Each sample (50 mg) was first heated at 423 K in a Ar flow (80 $cm^3min^{-1}$) until no change of weight was detected. Then, the sample was heated in a 5 vol%$H_2$/Ar flow (80 $cm^3min^{-1}$) from this temperature to 1173 K at 5K $min^{-1}$ and maintained at 1173 K until the reduction process was finished.

**Scanning electron microscopy (SEM)**

Scanning electron micrographs were obtained with a JEOL JSM6400 scanning microscope operating at accelerating voltages in the range 30-35 kV, work distances (wd) between 7-9mm and magnification values in the range 7000-50000x.

## RESULTS AND DISCUSSION

### MgO characterization

The results of characterizing the different magnesium oxides used can be seen in Table 1. Powder diffraction patterns of the MgO samples showed diffraction peaks at 2θ angles and relative intensities that can be indexed to a MgO periclase phase for the three samples. Very low amounts of other phases were also observed for the sample $MgO_{C1}$. They were identified as $Al(OH)_3$ and $Mg_5(CO_3)_4(OH)_2.2H_2O$ phases.

**TABLE 1**

**Characterization of MgO**

| Samples | $MgO_{C1}$ | $MgO_N$ | $MgO_A$ |
|---|---|---|---|
| Crystalline phases (XRD) | MgO mainly $Al(OH)_3$ $Mg_5(CO_3)_4(OH)_2.2H_2O$ | MgO | MgO |
| MgO crystallite sizes (nm)[a] | 46.6 | > 120 | 24.7 |
| Surface area ($m^2g^{-1}$)[b] | 223.0 | 2.5 | 49.9 |

[a] Using Scherrer equation.

[b] Using BET areas method.

Sample $MgO_N$ has the lowest BET area (2.5 $m^2g^{-1}$) which corresponds to the largest (> 120 nm) crystallite size (determined by the Scherrer equation from the diffraction data). Sample $MgO_{C1}$ ,which has

a higher BET area (223 $m^2g^{-1}$), has a smaller crystallite size (46.6 nm) than that mentioned above. As observed, these two samples show a good correlation between the BET area and crystallite size values. On the other hand, sample $MgO_A$ has an intermediate BET area (49.9 $m^2g^{-1}$) whereas its crystallite size is lower (24.7 nm) than the expected value. This can be explained by the presence of an important agglomeration of small crystallites (as confirmed later by SEM) since these small crystallites constitute the diffraction domain.


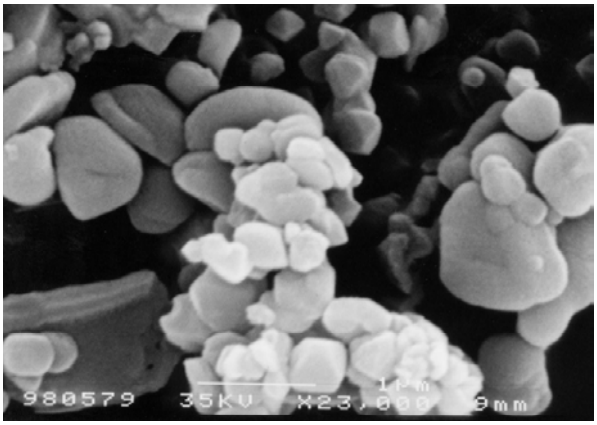

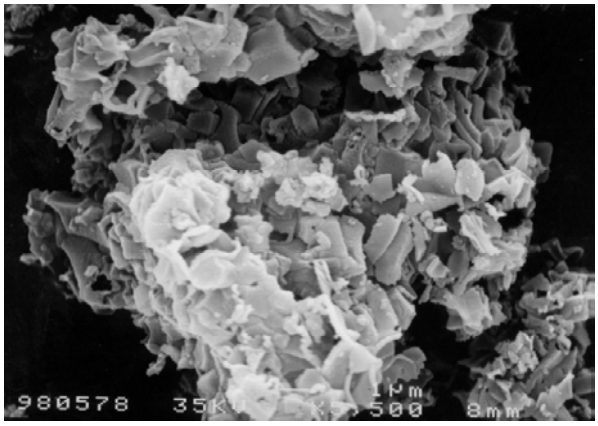


**FIG. 1.** Scanning electron micrographs of the MgO samples: (a) $MgO_{C1}$, (b) $MgO_N$, (c) $MgO_A$.

Fig.1 shows the micrographs of the three MgO. Samples $MgO_{C1}$ and $MgO_A$ have a layered appearance whereas sample $MgO_N$ has particles with non homogeneous morphologies (round, elongated and geometrical) and sizes between 1200 nm and 300 nm. The layered forms are more sintered for the sample $MgO_A$. This is in agreement with the lowest crystallinity as observed by XRD for this sample.

**NiO-MgO characterization**

***Controlled thermolysis study***

In previous studies [18], we observed that the formation of a single $Ni_3(NO_3)_2(OH)_4$ phase by controlled decomposition from the nickel nitrate hexahydrate, leads to (after calcination) homogenous octahedral particles of NiO around 200 nm.

In order to study the sequence of formation of this $Ni_3(NO_3)_2(OH)_4$ as a single phase in the presence of the different magnesia, we performed three decomposition experiments at different temperatures. We always used a homogeneous physical mixture of $Ni(NO_3)_2.6H_2O$ and one of the three magnesia ($MgO_{C1}$, $MgO_N$ and $MgO_A$). Each mixture was then heated and its evolution was studied by XRD.

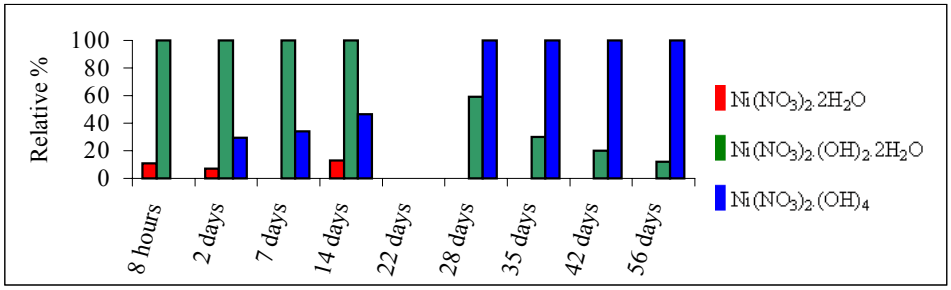


1. $Ni(NO_3)_2.6H_2O$ / $MgO_{C1}$.

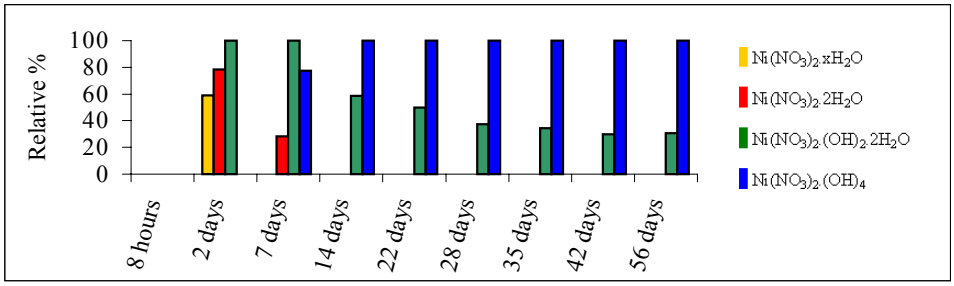


2. $Ni(NO_3)_2.6H_2O$ / $MgO_N$.
3. $Ni(NO_3)_2.6H_2O$ / $MgO_A$.

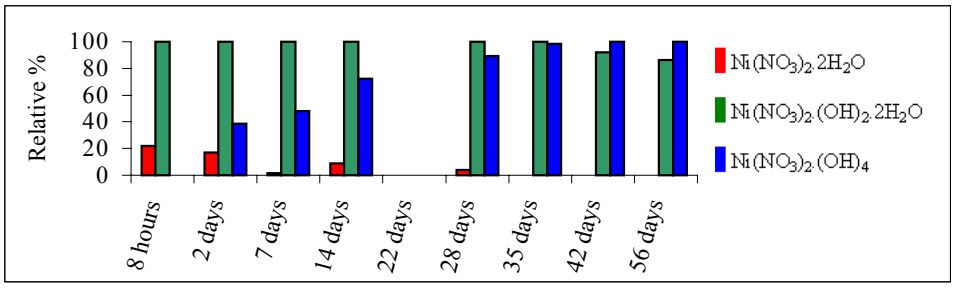


**FIG. 2.** Evolution of the crystalline phases at 403 K in front of the decomposition time for three $Ni(NO_3)_2.6H_2O$ / MgO mixtures.

*A) Samples heated at 373 K for 8 hours and for 2, 4, 7, 14, 21 and 28 days.*

No $Ni(NO_3)_2.6H_2O$ phase was observed in any of the samples but a crystalline phase, not described previously in the literature about this decomposition reaction, was detected in different relative proportions for all. This new phase, that we call $Ni(NO_3)_2.xH_2O$, could not be identified with the JCPDS files consulted.

The powder diffraction pattern of the sample after 8 hours shows three peaks which correspond to this $Ni(NO_3)_2{\cdot}xH_2O$ phase (in the highest amount) and two other phases identified as $Ni(NO_3)_2{\cdot}2H_2O$ and $Ni_2(NO_3)_2(OH)_2{\cdot}2H_2O$. This may lead us to think that the $Ni(NO_3)_2{\cdot}xH_2O$ phase lies between 6<x>2. However, we observed that a $Ni(NO_3)_2{\cdot}4H_2O$ phase appeared as the main phase when the $Ni(NO_3)_2{\cdot}xH_2O$, obtained from the decomposition in the presence of $MgO_N$, was accidentaly exposed to a temperature 20 K lower (353 K). This $Ni(NO_3)_2{\cdot}4H_2O$ phase change into a $Ni(NO_3)_2{\cdot}xH_2O$ phase when the sample is again heated and it then evolves in the same way as mentioned above. These results permit to propose a "x" value between 4 and 2 for this new phase which is very probably the tetrahydrate specie in a non usual crystalline form. This is in agreement with the assignment proposed in the literature for these phases as 9, 6, 4 or 2 hydrate [19].

When the decomposition time increases, there is a decrease in the relative proportion of the $Ni(NO_3)_2{\cdot}xH_2O$ phase which is accompanied by a gradual increase in the $Ni(NO_3)_2{\cdot}2H_2O$ and $Ni_2(NO_3)_2(OH)_2{\cdot}2H_2O$ phases. It should be noted that the nickel nitrate hexahydrate decomposes faster in the $MgO_{C1}$ or $MgO_A$ mixtures than in $MgO_N$.

There are low amounts of the phase of interest, $Ni_3(NO_3)_2(OH)_4$, after 14 days of decomposition in the presence of $MgO_{C1}$ or $MgO_A$ and after 28 days if the decomposition takes place in the presence of $MgO_N$. Consequently, the temperature of decomposition must be increased to obtain this phase in less time.

From these results we can propose a sequence of decomposition of the nickel nitrate hexahydrate to $Ni_3(NO_3)_2(OH)_4$, all mixed with MgO:

$$Ni(NO_3)_2.6H_2O \xrightarrow{\Delta} Ni(NO_3)_2.xH_2O \xrightarrow{\Delta} Ni(NO_3)_2.2H_2O \xrightarrow{\Delta} Ni_2(NO_3)_2(OH)_2.2H_2O \xrightarrow{\Delta} Ni_3(NO_3)_2(OH)_4$$

$$Ni(NO_3)_2.xH_2O \rightleftarrows Ni(NO_3)_2.4H_2O$$

This sequence is basically in agreement with the scheme of decomposition of pure nickel nitrate hexahydrate described elsewhere [19].

*B) Samples heated at 403 K for 8 hours and for 2, 4, 7, 14, 22, 28, 35, 42 and 56 days.*

Fig. 2 shows the relative evolution of the different phases in front of the decomposition time for the three $Ni(NO_3)_2{\cdot}6H_2O$/MgO mixtures. In the first two days, after the decomposition of the nickel nitrate with $MgO_{C1}$ or $MgO_A$, the $Ni_2(NO_3)_2(OH)_2{\cdot}2H_2O$ and $Ni_3(NO_3)_2(OH)_4$ phases were predominantly obtained. In the presence of $MgO_N$, on the other hand, the $Ni(NO_3)_2{\cdot}xH_2O$, $Ni(NO_3)_2{\cdot}2H_2O$ and $Ni_2(NO_3)_2(OH)_2{\cdot}2H_2O$ phases were detected for the same decomposition time as the samples mentioned above. Therefore, the initial

decomposition evolves faster in the presence of $MgO_{C1}$ or $MgO_A$ than in the presence of $MgO_N$.

However, all three samples evolve slowly to $Ni_3(NO_3)_2(OH)_4$ as a single phase. The proportions of this phase are highest when using $MgO_{C1}$ and lowest when using $MgO_A$. There are practically no changes in the relative proportions after day 28 for the mixtures with $MgO_N$ or $MgO_A$. The lower proportion observed for the sample with $MgO_A$ could be due to changes produced in the texture of the sample during the decomposition process since initially there was a rapid evolution of the phases. The highest tendency of the $MgO_A$ to form agglomerates (as confirmed by XRD and BET results) hinders the elimination of decomposition products over time. On the other hand, the nickel nitrate in the presence of $MgO_{C1}$ has a slow but progressive decomposition.

*C) Samples heated at 433 K for 2, 4, and 7 days.*

The three different mixtures show the same crystalline phases: $Ni_2(NO_3)_2(OH)_2.2H_2O$ and $Ni_3(NO_3)_2(OH)_4$ after 2 and 4 days and only the $Ni_3(NO_3)_2(OH)_4$ phase after 7 days. As expected, a high decomposition temperature leads faster to the formation of the $Ni_3(NO_3)_2(OH)_4$ phase as a single phase.

**BET areas**

Table 2 shows the BET areas for the $Ni_3(NO_3)_2(OH)_4$-MgO precursors obtained by thermolysis at 433 K for 7 days (path B). On the whole, all the values are similar and low (12-20 $m^2g^{-1}$). However, these values can be correlated with the areas of the magnesias used to prepare each sample. The precursors with the highest and the lowest

areas are those obtained from the commercial magnesia ($MgO_{C1}$) and the magnesia obtained from magnesium nitrate ($MgO_N$), respectively.

The mixtures with $MgO_{C1}$ and $MgO_A$ lose a considerable amount of area in comparison to the corresponding magnesias because of the agglomeration processes which take place in the presence of water vapour.

**TABLE 2**

**Characterization of the MgO-NiO precursors prepared by path B): P4C$_1$B, P4NB, P4AB**.

| Samples | P4C$_1$B | P4NB | P4AB |
|---|---|---|---|
| Crystalline phases (XRD) | $Ni_3(NO_3)_2(OH)_4$ | $Ni_3(NO_3)_2(OH)_4$ | $Ni_3(NO_3)_2(OH)_4$ |
| Crystallite sizes (nm)[a] | 21.2 | 32.0 | 24.7 |
| Surface area ($m^2g^{-1}$)[b] | 19.1 | 12.3 | 14.7 |

[a] Using Scherrer equation.

[b] Using BET areas method.

Table 3 shows the BET areas obtained for the different NiO-MgO systems prepared. Independently of the different magnesias, the weight ratio of NiO/MgO and the preparative path used, these samples have very similar area values.

These areas are also similar to the areas of NiO obtained from the thermal decomposition of the nickel nitrate hexahydrate [18]. These results are in agreement with those reported by Anderson et al. [17]

who observed a great sintering of high-area magnesias in the presence of low amounts of water vapour at the calcination temperatures used.

**TABLE 3**

**Characterization of systems NiO-MgO.**

| Samples | $4C_1A$ | $4C_1B$ | 4NA | 4NB | 4AB | 1NA | $1C_1A$ |
|---|---|---|---|---|---|---|---|
| Crystalline phases (XRD) | NiO-MgO | NiO-MgO | NiO-MgO | NiO-MgO | NiO-MgO | NiO-MgO | NiO-MgO |
| Surface area ($m^2g^{-1}$)[a] | 31.9 | 35.7 | 24.5 | 17.5 | 23.8 | 29.4 | 27.0 |

[a] Using BET areas method.

However, if the magnesia is varied for a NiO/MgO weight ratio of 4, we can observe some small diferences as a function of the preparative procedure followed. Samples prepared by path B with $MgO_N$ or $MgO_A$ have lower areas than those prepared by path A whereas when $MgO_{C1}$ is used, the sample with the lowest area is the one prepared by path A. The samples with $MgO_{C1}$ behave as expected because the calcination temperature of path B is lower (523 K) than the calcination temperature of path A (673 K). Nevertheless, and as the decomposition study which was carried out to obtain the precursor $Ni_3(NO_3)_2(OH)_4$ showed, the use of $MgO_N$ or $MgO_A$ hinders the elimination of the decomposition products which explains the higher tendency of these magnesias to sinter in the presence of water. If the calcination temperature is low, the water vapour pressure in the medium will be high. Therefore, sintering will be higher and the samples obtained by path B will have lower BET areas.

**Scanning electron microscopy (SEM)**

Scanning electron microscopy was used to monitor the morphology and particle size for the different NiO-MgO systems. Fig. 3, 4 and 5 show the micrographs of the samples $4C_1A$ and 4NA; $4C_1B$, 4NB and 4AB; $1C_1A$ and 1NA, respectively.

For the systems with a NiO/MgO weight ratio of 4, paths A and B lead to samples which have different morphologies and particle sizes (figs. 3 and 4). As observed, the samples prepared by path B have smaller particles (around 100 nm) and are more homogeneous than the samples prepared by path A (the particle size ranges between 100 and 1000 nm).

**a)**

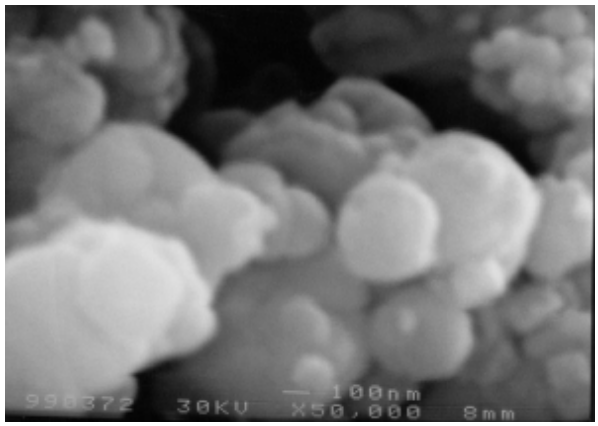

**b)**

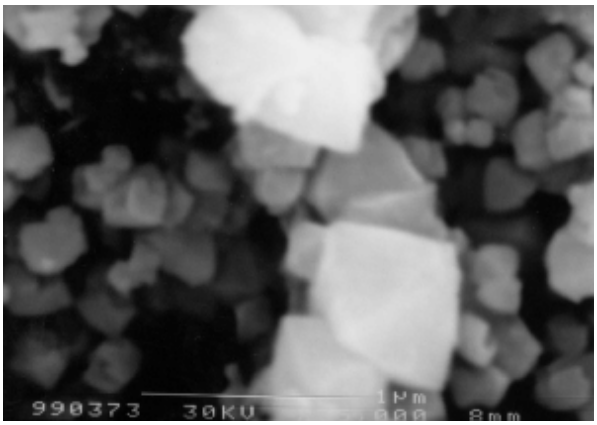


**FIG. 3.** Scanning electron micrographs of NiO-MgO systems with weight ratio 4:1 prepared by path A: a) $4C_1A$ and b) 4NA.

Sample 4NA has particles with octahedral morphology whereas the particles of sample $4C_1A$ are rounded and have an agglomerated and less crystalline appearance (fig.3).

**a)**

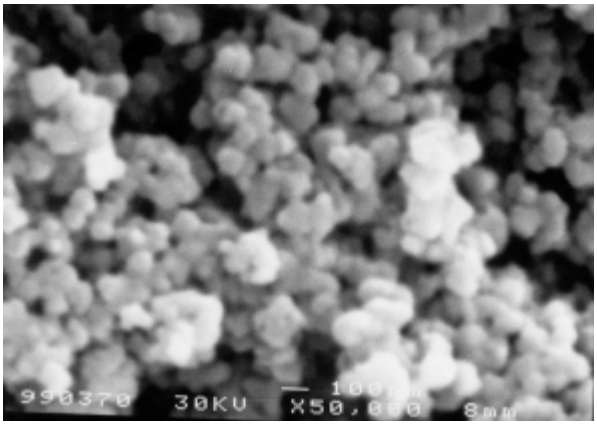

**b)**

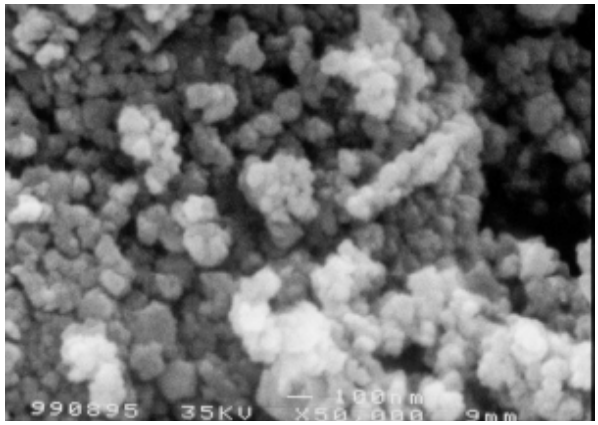


**c)**

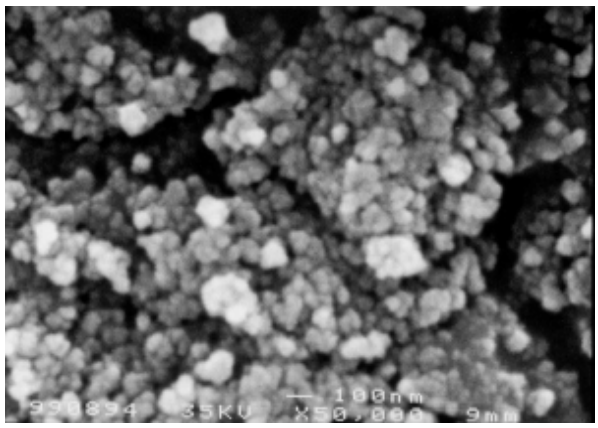


**FIG. 4.** Scanning electron micrographs of NiO-MgO systems with weight ratio 4:1 prepared by path B: a) $4C_1B$, b) 4NB and c) 4AB.

The micrographs of 4NB and 4AB (fig. 4) show greater sintering than the one prepared from path A (4NA) but sample $4C_1B$ seems to be less agglomerated than $4C_1A$. These results agree with the data of crystallinity obtained by XRD and BET area values mentioned above.

**a)**

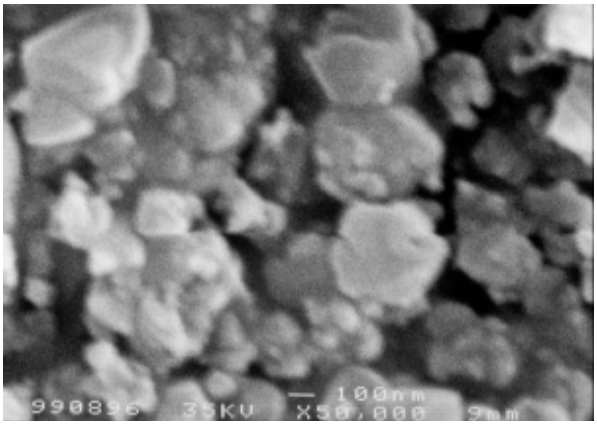


**b)**

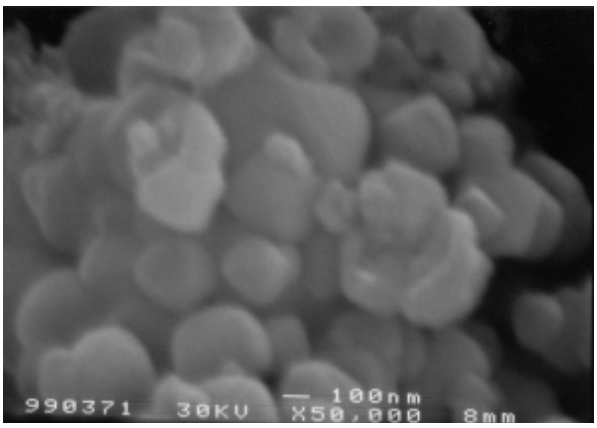


**FIG. 5.** Scanning electron micrographs of NiO-MgO systems with weight ratio 1:1: a) $1C_1A$ and b) 1NA.

The systems with NiO/MgO weight ratio of 1 (fig. 5) exhibit heterogeneous agglomerated particles. From these results, we can confirm that the use of path B led to NiO-MgO systems more homogeneous than the use of path A.

**X-ray diffraction (XRD)**

Powder diffraction patterns of the NiO-MgO systems, showed diffraction peaks at 2θ angles and relative intensities that can be indexed to a crystalline solid solution phase. The XRD patterns of this solid solution phase are very similar to those of NiO and MgO alone.

The diffraction lines for the faces (2 2 0), (3 1 1) and (2 2 2) can be used to identify the formation of a solid solution, because their lower intensity and greater sensitivity show deformations, due to the presence of NiO or MgO as different phases.

The peaks corresponding to the 2θ angles associated to the formation of solid solution, were well defined for all samples. This indicates that the use of magnesia with different surface properties, modifications in the preparative method and the calcination temperatures have not significative influence on the formation of the solid solution. No unreacted NiO was detected.

The slight differences observed in the BET area values (Table 3) are in agreement with the observation that the cristallinity of all the NiO-MgO systems was similar.

**Temperature-programed reduction (TPR)**

In order to study comparatively the reducibility of the NiO-MgO systems, the reduction degree α (expressed as $W_o$-$W_t$/$W_o$-$W_f$, where $W_o$ is the weight of the unreduced sample, $W_t$ is the weight of the sample given at temperature $_t$ and $W_f$ represents the weight of the completely reduced sample) was calculated for all the samples at different temperatures. The results are shown in Table 4.

We observed that the interaction between NiO and MgO leads to a NiO-MgO solid solution for all samples. We assume the formation of a solid solution in two steps: firstly, there is a surface diffusion of NiO and MgO phases and, secondly, there is a diffusion inside of both lattices. This diffusion mechanism is in agreement with what was reported by Arena et al. [22-23].

By studying the first derivative, we observed wide bands for all the systems which are probably related to a continuous modification of the NiO-MgO ratio. The systems with a NiO/MgO weight ratio of 1 (table 4) have a lower degree of reduction and a higher initial reduction temperature than the systems with a NiO/MgO weight ratio of 4. This is because the initial reduction temperature and the number of reduction steps depend on the amount of MgO. Ruckenstein et al. [13] found that the electronic transfer from NiO to MgO in solid solutions involves strong interactions between NiO and MgO and this inhibits the reduction of NiO.

In the systems with a NiO/MgO weight ratio of 4, the use of preparative path A gives lower reduction degrees than path B. However, the highest initial reduction temperatures were obtained for samples $4C_1A$ and 4NB (see table 4).

These reduction degrees may be due to the higher calcination temperature, 673 K instead of 523 K, used in path B. Consequently, there is a better diffusion between the NiO and MgO phases. Nevertheless, the fact that sample 4NA has a higher BET area value than sample 4NB (see table 3) could favour the reduction process to start at a lower temperature.

**TABLE 4**

**Reduction degree (α) of the systems NiO-MgO obtained by TPR.**

| Samples | $4C_1A$ | $4C_1B$ | 4NA | 4NB | 4AB | 1NA | $1C_1A$ |
|---|---|---|---|---|---|---|---|
| $T_R$(K)[a] | 613 | 604 | 598 | 647 | 605 | 679 | 649 |
| α ( 773) | 0.12 | 0.2 | 0.07 | 0.41 | 0.24 | 0.03 | 0.01 |
| α ( 873) | 0.33 | 0.42 | 0.37 | 0.78 | 0.48 | 0.15 | 0.10 |
| α ( 973) | 0.58 | 0.68 | 0.64 | 0.93 | 0.73 | 0.37 | 0.36 |
| α (1073) | 0.78 | 0.89 | 0.86 | 0.97 | 0.90 | 0.65 | 0.65 |
| α (1173) | 0.91 | 0.99 | 0.98 | 0.99 | 0.97 | 0.90 | 0.85 |

[a] $T_R$: Initial reduction temperature.

The use of different magnesia and preparative paths affects the reducibility of the systems. For the samples prepared by path A, the initial reduction temperature is higher when the commercial magnesia is used than when the magnesia obtained from magnesium nitrate is used. As expected, the lower the initial reduction temperature, the higher the reduction degree.

On the other hand, when path B was used, the system prepared from the magnesia $MgO_{C1}$ had a lower initial reduction temperature and also a lower reduction degree than that prepared from $MgO_N$. The system with magnesia $MgO_{C1}$ has a higher BET area (see table 3) than the system with magnesia $MgO_N$. This explains the lowest initial reduction temperature observed for sample $4C_1B$. Difussion may be lower between NiO-MgO phases in system 4NB because the crystallites are larger. This may be the reason why the degree of reduction is higher.

## CONCLUSIONS

Several NiO-MgO systems were prepared by varying the magnesia source, the NiO/MgO weight ratio and the preparative method. By path A, $Ni(NO_3)_2.6H_2O$ was directly transformed into NiO whereas by path B the transformation took place in two steps: first, $Ni(NO_3)_2.6H_2O$ was transformed into $Ni_3(NO_3)_2(OH)_4$ and then, this phase was transformed into NiO. All the samples were structurally characterized by using BET, XRD, SEM and TPR techniques.

The decomposition sequence of the nickel nitrate hexahydrate in the $Ni(NO_3)_2{\cdot}6H_2O$-MgO systems, observed from a controlled thermolisis study, was similar to that reported for the nickel nitrate hexahydrate without magnesia.

The initial velocities of decomposition of all the samples studied were fast although the intermediate hydroxylated species formed most rapidly for the system with commercial magnesia ($MgO_{C1}$). $Ni_3(NO_3)_2(OH)_4$ formed as a single phase by heating at 433 K for seven days, independently of the magnesia used.

XRD was used to identify the solid solutions obtained for all the NiO-MgO systems prepared. The BET results showed that there were no great differences in the area values, which were slightly higher for the systems prepared with $MgO_{C1}$.

The micrographs obtained by SEM showed that the crystalline morphologies and particle sizes depended on which preparative path, A or B, was used. The NiO-MgO prepared by path B gave a homogeneus system with agglomerated crystallites of sizes around 100 nm. This confirms that the intermediate formation of the $Ni_3(NO_3)_2(OH)_4$ phase as

a precursor of the NiO is one way of controlling the morphology and obtaining more homogeneous systems.

TPR shows that the NiO-MgO samples have different reducibilities. The systems prepared with a NiO/MgO weight ratio of 4 have lower initial temperatures of reduction and higher degrees of reduction than those prepared with a ratio of 1. Path B provides the highest degrees of reduction.

**REFERENCES**

1. Razhork, and R. I., Mikhail, R. S., *J. Phys. Chem.* **63,** 1050 (1959).
2. Kotsev, N. K., and Ilieva, L. I., *Catal. Lett.* **18,** 173 (1993).
3. Bukovec, P., Bukovec, N., Orel, B., and Wissiak, K. S., *J. Therm. Anal.* **40,** 1193 (1993).
4. Medina, F., Salagre, P., Fierro, J. L. G., and Sueiras, J. E., *J. Catal.* **142,** 392 (1993).
5. Medina, F., Salagre, P., and Sueiras, J. E., *J.Chem. Soc. Faraday Trans.* **90**(10), 1455 (1994).
6. Cesteros, Y., Fernández, R., Estellé, J., Salagre, P., Medina, F., Sueiras, J. E., and Fierro, J. L. G., *Appl. Catal. A: Gen.* **152**, 249 (1997).
7. Cesteros, Y., Salagre, P., Medina, P., and Sueiras, J. E. *Appl. Catal. B: Environ.* **22,** 135 (1999).
8. Morato, A., Alonso, C., Medina, F., Salagre, P., Sueiras, J. E., Terrado, R., and Giralt, A., *Appl. Catal. B: Environ.* **23**, 175 (1999).
9. Rathouský, J., Zukal, A., and Stárek, J., *Appl. Catal. A* **94,** 167 (1993).

10. Schaper, J. J. Berg-Slot, and W. H. J. Stork, Appl. Catal. **54,** 79 (1989).

11. Thomasson, P., Tyagi, O. S., and Knözinger, H., *Appl. Catal A* **181,** 181 (1999).

12. Parmaliana. A., Arena, F., Frusteri, F., Coluccia, S., Marchese, L., Martra, G., and Chuvilin, A. L., *J. Catal.* **141**, 34 (1993).

13. Ruckenstein, E., and Hang Hu, Y., *Appl. Catal. A* **183**, 85 (1999).

14. Smirniotis, P. G., and Zhang, W., *Appl. Catal A* **176**, 63 (1999).

15. Bhattacharyya, A., and Chang, W. W., "Catalyst Deactivation, Studies in Surface Science and Catalysis", (Delmon, B., and Froment, G.F., Ed.), Vol. 88, Elsevier, Amsterdam, 1994.

16. Kang, Y. C., Park, S. B., and Kang, Y. W., *Nanostruct. Mater.* **5**, 777 (1995).

17. Anderson, P. J., and Hohrlock, R. F., *Trans. Faraday Soc.* **58**, 1993 (1962).

18. Estellé, J., Doctoral Thesis, Rovira i Virgili University, Tarragona 1997.

19. Paulik, F., Paulik, J., and Arnold. M., *Thermochim. Acta* **121**, 137 (1987).

20. Elmasry, M. A. A., Gaber, A., and Khater, E. M. H., *J.Therm. Anal.* **52**, 489 (1998).

21. Llewellyn, P. L., Chevrot, V., Ragaï, J., Cerclier, O., Estienne, J., and Rouquérol, F., *Solid State Ionics* **101**, 1293 (1997).

22. Parmaliana, A., Arena, F., Frusteri, F., and Giordano, N., *J. Chem. Soc. Faraday Trans.* **86**(14), 2663 (1990).

23. Arena, F., Frusteri, F., Parmaliana, A., Plyasova, L., and Shmakov, A. N., *J. Chem. Soc., Faraday Trans.* **92**, 469 (1996).

24. Arena, F., Frusteri,F., and Parmaliana, A., *Appl. Catal. A* **187,** 127 (1999).

**IV.1.4 Desarrollo de vías preparativas para obtener sistemas NiO-MgO con diferente grado de interacción entre las fases.**

*Solid State Ionics, Pendiente de aceptación*



Influence of the interaction between phases on the properties of NiO-MgO samples.

Marc Serra[a], Pilar Salagre[a*], Yolanda Cesteros[a], Francisco Medina[b] and Jesús E. Sueiras[b].

*[a] Facultat de Química, Universitat Rovira i Virgili, Pl. Imperial Tarraco,1. 43005, Tarragona, Spain. e-mail:salagre@quimica.urv.es*

*[b] Escola Tècnica Superior d'Enginyeria Química, Universitat Rovira i Virgili,*

*Pl. Imperial Tarraco,1. 43005, Tarragona, Spain*

**ABSTRACT**

Several NiO-MgO samples were prepared from commercial nickel nitrate hexahydrate and MgO by means of different preparative paths and with two NiO/MgO weight ratio of 1 and 4. All the samples were structurally characterized using BET, XRD, SEM and TPR techniques. These preparative paths lead to NiO-MgO samples with different interaction level between NiO and MgO phases, which goes from the formation of solid solution until the detection of clearly differentiated phases by XRD. It is possible to obtain NiO/MgO samples with high surface area (80-90 $m^2g^{-1}$) by using an argon flow passing through the sample during the decomposition of the intermediate $Ni_3(NO_3)_2(OH)_4$ phase. The use of this precursor induces, during the calcination process, the formation of an oxide with octahedral morphology. Nevertheless, when there is a high interaction between NiO and MgO phases an also when there is a higher amount of magnesia (weight ratio of 1) the resolution of these octahedrons is lower. A higher interaction between NiO and MgO phases involves a higher initial NiO reduction temperature and, consequently a lower reduction degree.

*Key Words:* nickel nitrate hexahydrate, magnesium oxide; controlled thermal analysis, high-surface area NiO, solid solution, nickel oxide reducibility, NiO/MgO.

**INTRODUCTION**

The properties of nickel and magnesium oxides and their applicability as catalysts have been widely studied [1-6]. In its reduced form, nickel oxide has been mainly used for reactions such as the hydrogenation of nitriles [7-10] and the hydrodechlorination of polychloroaromatic compounds [11,12].

On the other hand the magnesium oxide has been directly used as catalytic support [13-17], and as basic catalyst [18]. Some of the most important reactions in which MgO is involved are reactions such as aldolic condensation, isomerization of double bonds [19], methane steam reforming and other light hydrocarbons [14-15], ethane partial oxidation [20,21], oxidative methylation of acetonitrile [22], and hydrogenation of cetones [23].

The key factor in obtaining oxides with different properties has been the use of different preparative methods [24-27].The decomposition of nickel nitrate hexahydrate is a procedure which has been widely studied [27-29], and which can be performed under controlled conditions of water pressure to obtain the nickel nitrate anhydrous as the direct precursor of NiO. The NiO obtained by this method has much higher area (around 50 $m^2g^{-1}$) than the NiO formed by decomposition in stationary air (around 1 $m^2g^{-1}$) using a basic nitrate as precursor [30].

On the other hand, we reported in previous studies [27], that the formation of a single phase $Ni_3(NO_3)(OH)_4$, by controlled decomposition from the nickel nitrate hexahydrate, leads to (after calcination) homogeneous octahedral particles of NiO around 200-300 nm. However, the controlled decomposition of $Ni(NO_3)_2.6H_2O$ in the presence of different sources of magnesia until the formation of the single phase $Ni_3(NO_3)(OH)_4$ showed a homogeneous system with agglomerated crystallites of sizes around 100 nm, but the octahedral morphology was not clearly defined. [31]

A high-area magnesia (> 200 $m^2g^{-1}$), can be prepared by calcination of magnesium hydroxide under vacuum. When these precursors are calcined in air, the area of the MgO obtained is often low. This is mainly due to the sintering phenomena that takes place in the presence of water vapour [13]. Incorporating divalent cations (Ni, Cu and Zn), preferably during the development of the surface area, is a good method of stabilizing the area of the magnesias prepared [13].

A considerable number of works have been focused on the study of the physical and chemical properties of the NiO-MgO system [31-33]. On the whole, it is accepted that the reactivity is highly affected by the tendency to form solid solutions [34]. Parmaliana et al. [34-36] reported the influence of the calcination temperature and the (%) nickel weight on the structure and morphology of the mixed systems. They also pointed out that the formation of solid solutions decreases the reducibility of the NiO phase.

Owing to the economic importance of preparing different Ni/MgO catalysts with different structural properties to be used in

different reactions, as reflected by the registration of numerous patents [37-42], much research has been carried out in last years. The aim of this work is to propose different synthesis procedures in order to obtain different interaction degrees between NiO and MgO phases. Also, we want to study the key factors that affect the structural and surface properties as the reducibility of NiO-MgO samples, in order to control the nickel oxide morphology and its surface properties.

## EXPERIMENTAL

### Samples preparation

Four different preparation procedures (A, B, C, and D) and two NiO/MgO weight ratios (1 and 4) were used to synthesize several NiO-MgO samples.

Commercial nickel nitrate hexahydrate (Panreac 99%) and commercial magnesia (Aldrich 99% 325 mesh, BET area of 114.9 $m^2g^{-1}$ and crystallite size of 13.9 nm, referred to as $C_2$) have been used for all procedures.

Path A) Two homogeneous physical mixtures of $Ni(NO_3)_2.6H_2O$ and MgO in the appropriate amounts were prepared. Then, the samples were calcined under air at 673 K for 4h (referred to as $1C_2A$ and $4C_2A$ for a weight ratio 1 and 4, respectively).

Path B) Two homogeneous physical mixtures of $Ni(NO_3)_2.6H_2O$ and MgO were submitted to a controlled thermolysis at 433 K for 14 days in order to obtain $Ni_3(NO_3)_2(OH)_4$ as single phase. These precursors were later calcined under air at 573 K for 4 h (samples 1 $C_2B$ and 4 $C_2B$).

Path C) In this procedure, the first step was a thermal decomposition of nickel nitrate hexahydrate at 373 K for 14 days until the formation of the basic species $Ni_3(NO_3)_2(OH)_4$ as single phase. This species was physically mixed with $MgO_{C2}$ in the appropriate amounts and subsequent calcined at 573 K flowing argon through the sample (300 $cm^3min^{-1}$) to obtain $1C_2C$ and $4C_2C$ samples.

Several experiments have been performed using this procedure in order to study the evolution of the surface area with the calcination time. Each sample was heated in a glass reactor from room temperature to 573 K at 5K $min^{-1}$, and maintained at this temperature for different times (8, 11, 13 hours).

Path D) First, the NiO phase was obtained by the thermal decomposition of nickel nitrate hexahydrate at 373 K for 14 days, until the formation of the basic species $Ni_3(NO_3)_2(OH)_4$ as single phase and later calcination at 573 K for 11 h, flowing argon through the sample (referred to as NiOB). Finally, two suspensions of this NiO and MgO in the weight ratio 1 and 4 were prepared with n-hexane by stirring for 24 h. The organic dissolvent was then evaporated and the homogeneous mixture NiO/MgO was obtained (samples $1C_2D$ and $4C_2D$).

**X-ray diffaction (XRD)**

Powder X-ray diffraction patterns of the different samples were obtained with a Siemens D5000 diffractometer using nickel-filtered Cu Kα radiation. Samples were dusted on double-sided sticky tape and mounted on glass microscope slides. The patterns were recorded over a range of 2θ angles from 10º to 90º and crystalline phases were

identified using the Joint Committee on Powder Diffraction Standards (JCPDS) files.

The XRD patterns of MgO are very similar to those of NiO. The peak positions corresponding to 2θ angles (with the relative intensities in parentheses), taken from the JCPDS files, are: 36.95 (10), 42.91 (100), 62.31 (52), 74.68 (4) and 78.61 (12) for the MgO phase and 37.28 (91), 43.30 (100), 62.92 (57), 75.44 (16) and 79.39 (13) for the NiO phase. Both 2θ peaks are assigned to the faces (1 1 1), (2 0 0), (2 2 0), (3 1 1) and (2 2 2), respectively.

**Surface areas, (BET method)**

Surface areas were calculated by the BET method from the nitrogen adsorption isotherms at 77 K using a Micromeritics ASAP 2000 surface analyser and a value of 0.164 $nm^2$ for the cross-section of the nitrogen molecule.

**Temperature-programmed reduction (TPR)**

Temperature-programmed reductions (TPR) were carried out in a Perkin Elmer TGA 7 microbalance equipped with a 273-1273 K programmable temperature furnace. The accuracy was ±1μg.

Each sample (20 mg) was first heated at 423 K in an Ar flow (80 $cm^3min^{-1}$) until no change of weight was detected. Then, the sample was heated in a 5 vol%$H_2$/Ar flow (80 $cm^3min^{-1}$) from this temperature to 1173 K at 5 K $min^{-1}$ and maintained at 1173 K until the reduction process was finished.

The reduction degree α, was expressed as $W_o$-$W_t$/$W_o$-$W_f$, where $W_o$ is the weight of the unreduced sample, $W_t$ is the weight of the sample given at temperature t and $W_f$ represents the weight of the completely reduced sample and was assigned as α=1.

**Thermogravimetric analyses (TGA)**

The thermogravimetric analyses (TGA) were carried out in a Perkin Elmer TGA 7 microbalance equipped with a 273-1273 K programmable temperature furnace. The accuracy was ±1μg.

Each sample (20 mg) was heated in a Ar flow (80 $cm^3min^{-1}$) from room temperature to 1173 K at 10 K $min^{-1}$ and maintained at 1173 K until no change of weight was detected.

**Scanning electron microscopy (SEM)**

Scanning electron micrographs were obtained with a JEOL JSM6400 scanning microscope operating at accelerating voltages in the range 30-35 kV, work distances (wd) between 9-15 mm and magnification values in the range 11000-45000x.

## RESULTS AND DISCUSSION

**Evolution of surface properties during the calcination process for the samples prepared by path C**

The different surface areas obtained for samples $1C_2C$ and $4C_2C$ at different calcination times are represented in Fig. 1.

There is an increase of surface area for both weight ratios by increasing the calcination time. However, XRD results only show the presence of the NiO phase for all samples and similar crystallite sizes for samples $1C_2C$ (between 14-16 nm)and for samples $4C_2C$ (18-19 nm). This similar surface area and lower crystallite size observed for samples $1C_2C$ than for samples $4C_2C$, could be due to the certain higher agglomeration of small particles since these small crystallites constitute the diffraction domain for samples $1\ C_2C$.

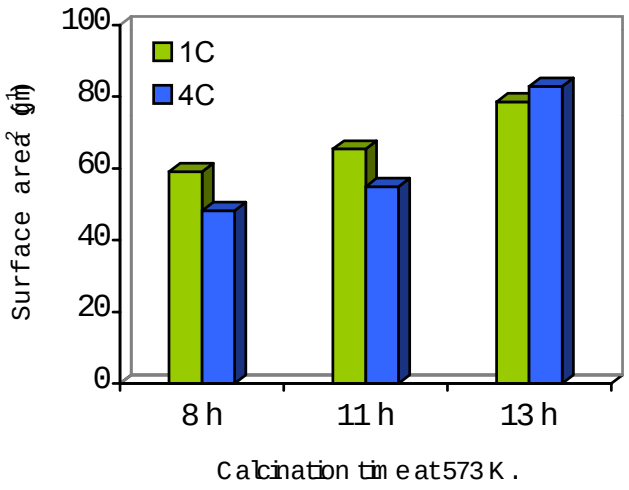


**FIG. 1.** Surface areas obtained for samples prepared by path C during the calcination process at 573 K for different times.

Several TGA experiments were performed under the conditions given in the experimental section in order to relate the surface area evolution with the presence of other phases. In all sample two weight losses were detected, the first one between room temperature and 673 K and the second one between 673 K and 873 K. This last loss (around

4-6 %) clearly corresponds to the loss of the non-stoichiometric oxygen of the sample which is corroborated with the colour change from black to green of each sample. The first loss is similar for all samples (4-6%). Therefore, the presence of residual non-crystalline precursor phase of NiO could be discarded. Probably, the water strongly adsorbed during the manipulation of sample could explain this loss.

In order to obtain more information about magnesia($C_2$), an experiment with magnesia and without nickel oxide was performed by heating at 573 K for 13 h in a glass reactor flowing argon through the sample. After this treatment there is an increase of the magnesia surface area until a value of 146 $m^2g^{-1}$. However, when magnesia is present during the decomposition process of $Ni_3(NO_3)_2(OH)_4$ it is submitted at water and/or nitrous vapours formed, and therefore an agglomeration process is favoured. This explains the disappearance of the crystalline periclase of XRD results.

Sample $4C_2C$ obtained at 8 and 11 h shows lower surface area values than the corresponding sample $1C_2C$ prepared at the same time. This can be related to a higher sintering suffered for sample $4C_2C$ than for sample $1C_2C$ which is probably due to the higher vapour amounts generated in proportion to the amount of magnesia phase for sample $4C_2C$ than for sample $1C_2C$. However, with the time, there is a certain disagglomeration of the phases for both samples due to the high argon flow which is passing through the sample and, finally, at 13 h similar surface areas are obtained (78.6 and 82.9 $m^2g^{-1}$ for sample $1C_2C$ and $4C_2C$, respectively).

**X-ray diffraction (XRD)**

Table 1 shows the characterization of the NiO-MgO systems prepared by different paths and a NiO sample prepared in the first step of path D.

Samples prepared by means of path A and B show diffraction peaks at 2θ angles and relative intensities that can be indexed to a crystalline solid solution phase (Table 1). The XRD patterns of this solid solution phase are very similar to those of NiO and MgO alone. The diffraction lines for the faces (2 2 0), (3 1 1) and (2 2 2) can be used to identify the formation of a solid solution because their lower intensity and greater sensitivity show deformations, due to the presence of NiO or MgO as different phases.

**TABLE 1**

**Characterization of the NiO-MgO systems and NiO sample.**

| | 1C$_2$A | 4C$_2$A | 1C$_2$B | 4C$_2$B | 1C$_2$C 13h | 4C$_2$C 13h | 1C$_2$D | 4C$_2$D | NiO B |
|---|---|---|---|---|---|---|---|---|---|
| Crystalline phases (XRD) | NiO-MgO solid solution | NiO-MgO solid solution | NiO-MgO solid solution | NiO-MgO solid solution | NiO | NiO | NiO MgO | NiO MgO | NiO |
| Crystallite sizes (nm)[a] | 28.9 | 27.3 | 18.5 | 24.1 | 15.4 | 17.8 | 27.7 (NiO) 12.6 (MgO) | 27.4 (NiO) 13.3 (MgO) | 27.1 |
| Surface area ($m^2g^{-1}$)[b] | 44.9 | 35.9 | 51.1 | 42.2 | 78.6 | 82.9 | 102.0 | 89.2 | 84.9 |

[a] Using Scherrer equation.

[b] Using BET area method.

On the other hand, samples synthesized by path C only show the diffraction peaks of the NiO phase. This is probably due to the use of an argon flow through the sample during calcination which could hinder the diffusion between the NiO and MgO phases. This is in agreement with Arena et al. who reported the importance of diffusion on the formation of a solid solution [35, 36]. The MgO periclase phase disappears probably as a consequence of the thermal treatment in presence of vapours, as commented above.

Finally, samples prepared by path D shows two phases: a crystalline NiO phase and a less crystalline peak that can be indexed to a MgO periclase phase. This indicates the expected lower interaction between these two phases for these samples.

**Surface areas, (BET method)**

The commercial magnesia used has high surface area (114.9 $m^2g^{-1}$). It is important to remark that this oxide in presence of air, evolves quickly to an agglomerated aspect with not well defined particles (Fig. 2a.). Table 1 shows the BET areas obtained for the different NiO-MgO systems prepared. Samples prepared by path A and B show similar area values and are in agreement with those reported by Anderson et al. [26] and last studies [31], which showed a great sintering of high-area magnesia in the presence of low amounts of water vapour at the calcination temperatures used. Therefore, these BET values are similar to the areas of NiO obtained from the thermal decomposition of the nickel nitrate hexahydrate [27].

Although the areas are similar, the samples prepared by means of path B, show values slightly higher than the samples prepared by path A. This is related to the higher calcination temperature used in

path A (673 K), and is in agreement with previous decomposition studies made with magnesias of high surface area [31]. Independently of the preparative path A or B, the samples prepared with a weigh ratio 1:1 of NiO-MgO have a bite more surface area, which indicates a lower sintering of the magnesia.

Samples prepared by path C and D have higher BET area than those prepared by path A and B. This can be explained in path C, by the use of an argon flow through the sample during calcination. This flow favours the efficient elimination of decomposition products and, therefore, the agglomeration effect is lower and probably also hinders the sintering of the NiO phase formed during the calcination process. The differences observed in the BET area values are in agreement with the observation of lower crystallite size for the samples prepared by path C.

However, the samples prepared by path D have similar crystallite sizes than the oxides alone and, therefore, the surface area corresponds to the proportional addition of the respective surface areas of the NiOB and $MgO_{C2}$ oxides. This is corroborated by its crystallite size, since NiO and MgO phases almost maintain the same crystallite size than before the suspension with n-hexane was made. This behaviour was expected due to the use of a dissolvent without water, which avoids the sintering of magnesia.

**Temperature-programmed reduction (TPR)**

In order to study comparatively the reducibility of the samples prepared from different preparative paths and with different weight ratios of NiO/MgO, the reduction degree $\alpha$ was calculated for all the samples at different temperatures. The results are shown in table 2.

**TABLE 2**

**Reduction degree ($\alpha$) achieved at different partial reduction temperatures for the systems NiO-MgO prepared by different paths and NiO B sample.**

| | 1C$_2$A | 4C$_2$A | 1C$_2$B | 4C$_2$B | 1C$_2$C 13 h | 4C$_2$C 13 h | 1C$_2$D | 4C$_2$D | NiO B |
|---|---|---|---|---|---|---|---|---|---|
| $T_R$ (K) [a] | 778 | 739 | 673 | 633 | 628 | 623 | 618 | 613 | 563 |
| $\alpha$ (773) | - | 0,03 | 0,11 | 0,21 | 0,76 | 0,80 | 0,85 | 0,92 | 1 |
| $\alpha$ (873) | 0,11 | 0,16 | 0,27 | 0,48 | 0,85 | 0,90 | 0,91 | 0,96 | 1 |
| $\alpha$ (973) | 0,29 | 0,36 | 0,48 | 0,71 | 0,92 | 0,95 | 0,94 | 0,98 | 1 |
| $\alpha$ (1073) | 0,51 | 0,60 | 0,70 | 0,88 | 0,96 | 0,98 | 0,97 | 1,00 | 1 |
| $\alpha$ (1173) | 0,77 | 0,85 | 0,90 | 0,98 | 0,99 | 1,00 | 0,99 | 1,00 | 1 |

[a] $T_R$ = initial reduction temperature.

The solid solution observed by XRD (NiO-MgO) for the samples prepared by paths A and B, lead to lower reduction degrees and higher initial reduction temperature than for those prepared by paths C and D. This is in agreement with the results of arena and Parmaliana et al. [34-36] and more recent studies [9-10, 31], which concluded that the formation of a solid solution hinders the reduction of the NiO phase. Studies of Ruckeintein and Hang Hu reported that the electronic transfer between NiO and MgO involves strong interaction, which inhibit the reduction of NiO [20].

Independently of the formation or not of a solid solution phase, the use of NiO/MgO with a weight ratio of 1 involves a higher initial reduction temperature and lower reduction degree than systems with a NiO/MgO weight ratio of 4. This indicates that the initial reduction temperatures depend on the amount of MgO.

Samples prepared by path A have the highest initial reduction temperature and the lowest reduction degree. This is related to a better diffusion between NiO and MgO phases for these sample obtained at the highest calcination temperature (673 K).

On the other hand, NiO/MgO systems prepared by paths C and D show similar initial reduction temperature and reduction degrees. However, analyzing the reduction experiment in more detail, we can observe that using the same weight ratio, the samples prepared by means of path C have lower initial reduction temperature and lower partial reduction degree at different temperatures than the samples prepared by path D. This is related to the higher dispersion of the magnesia by using path C, since when the nickel oxide is formed the magnesia is present. This favours a better diffusion between phases than in preparative D. However, it is not sufficient in order to form a solid solution probably due to the argon flowing through the sample. In

contrast, samples of path D become a mixture of oxides when they are already formed, so the diffusion between the phases could be something lower. This is corroborated by the presence of a crystalline MgO periclase phase, detected by XRD when path D was used. Interestingly, it is observed that NiO reduction is more difficult for the samples prepared by path D than for the NiOB alone sample. Also in this case, magnesia exercises an inhibitory effect in the reduction process.

**a)**

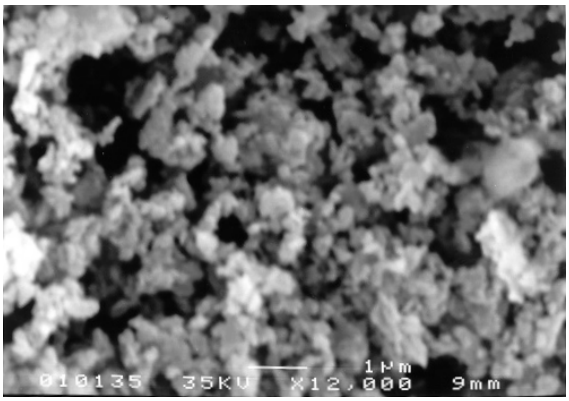


**b)**

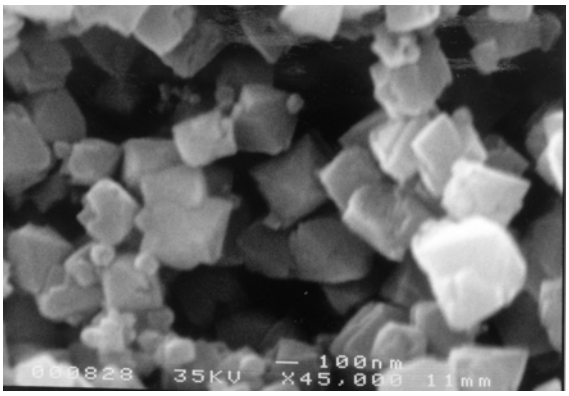


**Fig. 2.** Scanning electron micrograph of commercial $MgO_{C2}$ (a) and the NiOB sample (b).

**Scanning electron microscopy (SEM).**

Scanning electron microscopy was used to monitor the morphology and particle size for the different samples. Fig 2-6 show the micrographs of samples MgO,NiO (Fig. 2), 1 $C_2$A,4$C_2$A (Fig. 3), 1$C_2$B,4 $C_2$B (Fig. 4), 1$C_2$C,4$C_2$C prepared at 573 K 13 h (Fig. 5), and

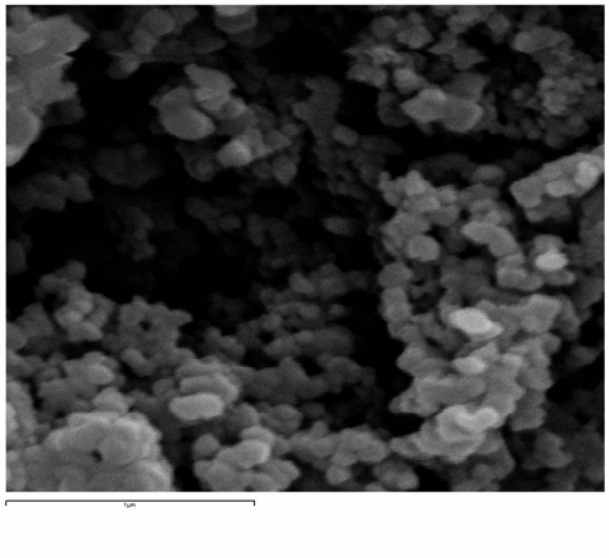

1$C_2$D,4$C_2$D (Fig. 6), respectively.

**Fig. 3.** Scanning electron micrograph of samples 1$C_2$A (a) and 4$C_2$A (b).

Samples prepared by means of the previously obtained $Ni_3(NO_3)(OH)_4$ phase (paths B, C and D), lead to the formation, after calcination, of particles with octahedral morphology.

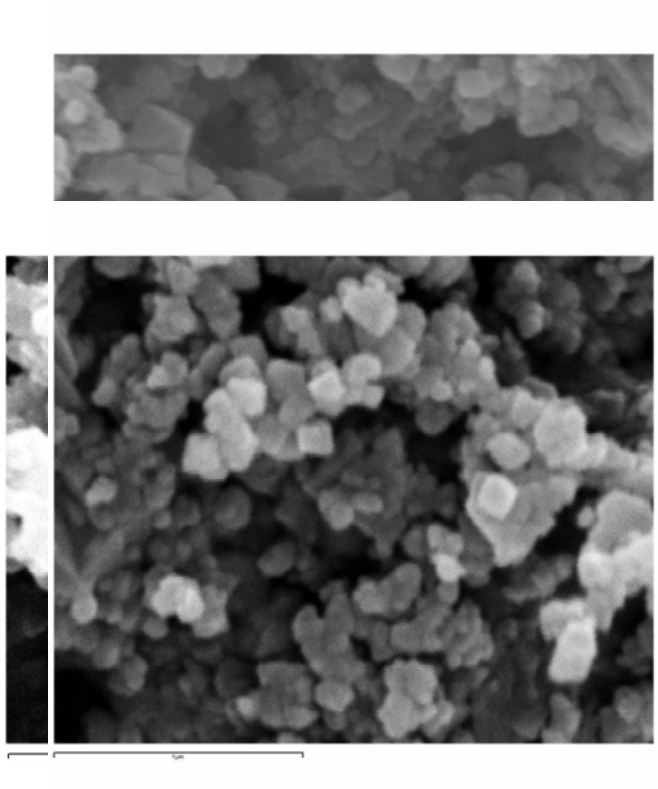

**Fig. 4.** Scanning electron micrograph of samples $1C_2B$ (a) and $4C_2B$ (b).

The NiOB obtained without the presence of magnesia shows the best octahedral resolution (Fig. 2b). Probably, without the MgO phase, the octahedrons formation is favoured.

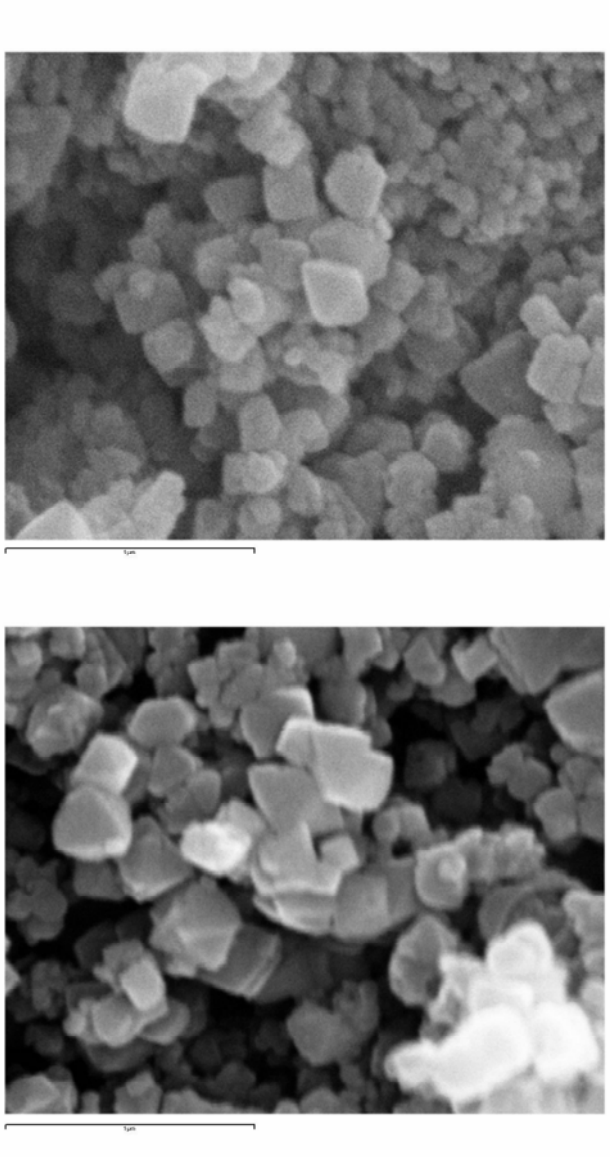

**Fig. 5.** Scanning electron micrograph of samples $1C_2C$ obtained at 573 K for 13h (a) and $4C_2C$ obtained at 573 K for 13h (b).

Samples prepared by paths C and D also show a better definition of particles than those prepared by path B, probably because of the less interaction between NiO-MgO phases. However, the samples which not form solid solution are also affected by the magnesia. Therefore, independently of the preparative path, the use of a higher amount of magnesia makes difficult the octahedral definition. This is corroborated since the use of 1 as NiO/MgO weight ratio, lead to a lower defined NiO particles that when a NiO/MgO weight ratio of 4 was

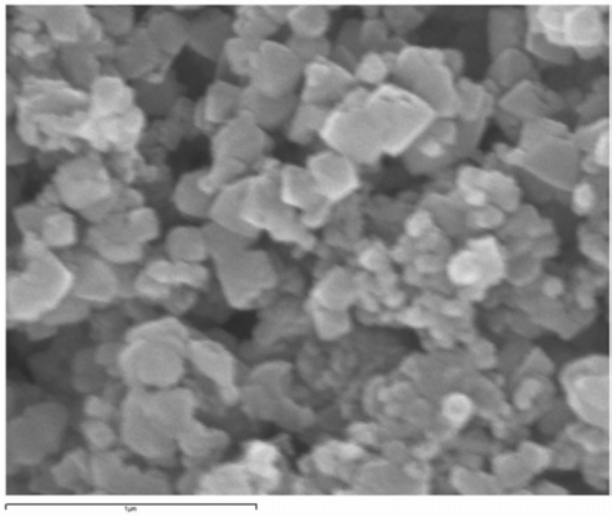

used.

**Fig. 6.** Scanning electron micrograph of samples 1 $C_2D$ (a) and $4C_2D$ (b).

## CONCLUSIONS

Several NiO-MgO systems with different structural and surface properties have been prepared by different paths and using two

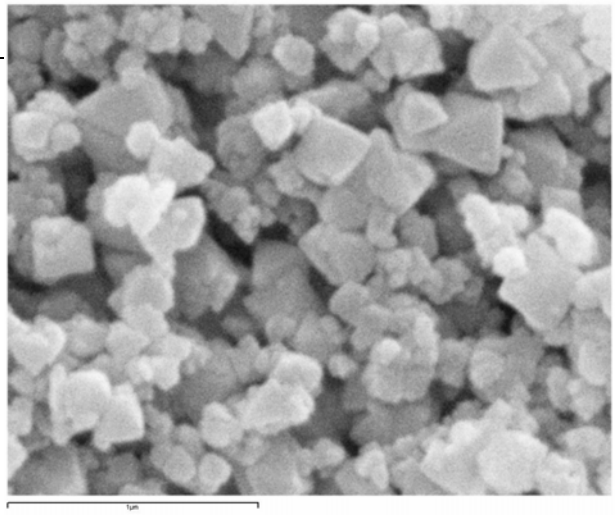

NiO/MgO weight ratios. All the samples were structurally characterized by using BET, XRD, SEM, and TPR techniques.

The decomposition of $Ni(NO_3)_2.6H_2O$ in the presence of magnesia (path A and B) leads to the formation of solid solution after calcination and, therefore, lower reduction degrees were obtained for these samples.

The calcination of $Ni_3(NO_3)_2(OH)_4$ / MgO under an argon flow passing through the sample (path C), gives place to systems with high surface area (around 80-90 $m^2g^{-1}$). This flow favours the efficient elimination of decomposition products. Therefore, the agglomeration effect is lower and probably also hinders the sintering of the NiO phase produced during the calcination process. Samples prepared by path C do not have solid solution and therefore the reduction is easier than samples obtained by path A and B.

The NiO/MgO formed by path D has a surface area corresponding to the proportional addition of the respective surface areas of the NiOB and $MgO_{C2}$ oxides used. This preparative path D produces a lower interaction between NiO and MgO phases than the others preparative paths. This was corroborated by the lowest initial reduction temperatures observed for the samples prepared by this path. However, the initial reduction temperature is higher than for a NiOB sample without magnesia.

Independently of the preparative path used, the use of a NiO/MgO weight ratio of 1 gives place to higher initial NiO reduction temperatures and therefore lower partial reduction degrees than when using a ratio of 4.

The use of precursor $Ni_3(NO_3)_2(OH)_4$, induces, during the calcination process, to the formation of an oxide with octahedral

morphology. Nevertheless, when there is a high interaction between NiO and MgO phases an also when there is a higher amount of magnesia (weight ratio of 1) the resolution of these octahedrons is lower.

**REFERENCES**

[1] Razhork, R. I., and Mikhail, R. S., *J. Phys. Chem.* **63**, 1050 (1959).

[2] Kotsev, N. K., and Llieva, L.I., *Catal Lett.* **18**, 173 (1993).

[3] Bukovec, P., Bukovec, N., Orel, B., and Wissiak, K. S., *J. Therm. Anal.* **40**, 1193 (1993).

[4] Biju, V., and Abdul-Khadar, M., *J. Mater. Sci.* **36**, 5779 (2001).

[5] Das, D., Pal, M., Di-Bartolomeo, E., Traversa, E., and Chakravorty, D., *J. Apll. Phys.* **88**, 6856 (2000).

[6] Christoskova, S. G., Stoyanova, M., Danova, N., and Argirov, O., *Appl. Catal. A:Gen.* **173**, 101 (1998).

[7] Medina, F., Salagre, P., Fierro, J. L. G., and Sueiras, J. E., *J. Catal.* **142**, 392 (1993).

[8] Medina, F. Salagre, P. and Sueiras, J. E., *J. Chem. Soc., Faraday Trans.* **90**,1455 (1994).

[9] Serra M., Salagre, P., Cesteros, Y., Medina, F., and Sueiras, J. E., *J. Catal.* **197**, 210 (2001).

[10] Serra M., Salagre, P., Cesteros, Y., Medina, F., and Sueiras, J. E., *J. Catal.* **209**, 202, (2002).

[11] Estellé, J., Ruz, J., Cesteros, Y., Fernandez, R., Salagre, P., and Sueiras, J. E., *J. Chem. Soc., Faraday Trans.* **92**, 2811 (1996).

[12] Morato, A., Alonso, C., Medina, F., Salagre, P., Sueiras, J. E., Terrado, and R., Giralt, A., *Appl. Catal.B:Environ.* **23**, 175 (1999).

[13] Schaper, H., Berg-Slot, J. J., and Stork, W. H. J., *Appl. Catal.* **54**, 79 (1989).

[14] Rathouský, J., Zukal, A., and Stárek, J., *Appl. Catal. A* **94**,167 (1993).

[15] Sidjabat, O., and Trimm, D. L., *Topics in Catalysis* **11/12**, 279 (2000).

[16] Klicpera, T., and Zdrazil, M., *Catal. Letters* **58**, 47 (1999).

[17] Dal Santo, V., Sordelli, L., Dossi, C., Recchia, S., Fonda, E., Vlaic, G., and Psaro. R., *J. Catal.* **198**, 296 (2001).

[18] Thomasson, P., Tyagi, O. S., and Knözinger, H., , *Appl. Catal. A: Gen.* **181**,181 (1999).

[19] Parmaliana. A., Arena, F., Frusteri, F., Coluccia, S., Marchese, L., Martra, G., and Chuvilin, A. L., *J. Catal.* **141**, 34 (1993).

[20] Ruckenstein, E., and Hang Hu, Y., *Appl. Catal. A: Gen.* **183**, 85 (1999).

[21] Bhatia, S., Zabidi, N. A. M., and Ahmad. M. H. A. M., *React. Kinet. Catal. Lett.* **74**(1), 87 (2001).

[22] Smirniotis, P. G., and Zhang, W., *Appl. Catal A: Gen.* **176**, 63 (1999).

[23] Sato, S., Takahashi, R., Sodesawa, T., Nozaki, F., Jin, X. Z., Suzuki, S., and Nakayama., T., *J. Catal.* **191**, 261 (2000).

[24] Kang, Y. C., Park, S. B., and Kang, Y. W., *Nanostruct. Mater.* **5**, 777 (1995).

[25] Thoms, H. Epple, M. Viebrock, H. and Reller, A., *J. Mater. Chem.* **5**(4),589 (1995).

[26] Anderson, P.J., Hohrlock, R. F., *Trans. Faraday Soc.* **58**, 1993 (1962).

[27] Estellé, J. PhD thesis, Rovira i Virgili University, Tarragona, Spain, 1998.

[28] Paulik, F. Paulik, J. and Arnold. M., *Thermochim. Acta* **121**, 137 (1987).

[29] Elmasry, M. A. A., Gaber, A., and Khater, E. M. H., *J.Therm. Anal.* **52**, 489 (1998).

[30] Llewellyn, P.L., Chevrot, V, Ragaï, J., Cerclier, O., Estienne, J., and Rouquérol, F., *Solid State Ionics* **101-103**, 1293 (1997).

[31] Serra M., Salagre, P., Cesteros, Y., Medina, F., and Sueiras, J. E., Solid State Ionics **134**, 229 (2000).

[32] Hagan, A. P., Lofthouse, M. G., Stone, F. S., and Trevethan, M. A., *"Preparation of Catalysts II"*, (Belnard D., Ed.), Elsevier, Amsterdam, 1979.

[33] Highfield, J. G., Bossi, A., and Stone F. S., "*Preparation of Catalysts III"*, (Poncelet, G., Grange., and Jacobs, P. A., Ed.), Elsevier, Amsterdam, 1983.

[34] Parmaliana, A., Arena, F., Frusteri, F., and Giordano, N., *J. Chem. Soc. Faraday Trans.* **86**(14), 2663, (1990).

[35] Arena, F. Fruster, F. Parmaliana, A. Plyasova, L. and Shmakov, A. N., *J. Chem. Soc., Faraday Trans.* **92**, 469 (1996).

[36] Arena, F. Frusteri, F. and Parmaliana, A., *Appl. Catal A:Gen.* **187**, 127 (1999).

[37] Kuniaki, N., Kazuhisa, F., Manabu, K., and Masayoshi. O., Japan Patent, JP5161848A2, 1993 (UBE IND LTD.).

[38] Dadong, L., Ying, H., and Yahua, S., China Patent, CN1085934A, 1994 (CHINA PETRO-CHEMICAL INDUSTRY CORP.).

[39] Akira, S., Hidetomo, N., Takehisa, F., and Kaori, S., Japan Patent, JP8071421A2, 1996 (CHUBU ELECTRIC POWER CO INC FINE CERAMICS CENTER).

[40] Deckers, G., Diekhaus, G., Dorsch, B:, Frohning, C. D., Horn, G., and Horrig, H. B., US Patent, US5498587, 1996 (HOECHST AKTIENGESELLSCHAFT).

[41] Jianming, H., Fuji, W., and Huijun W., China Patent, CN11411214A, 1997 (CATALYST PLANT, NANJING CHEMICAL INDUSTRY UP).

[42] Deckers, G., Diekhaus, G., Dorsch, B:, Frohning, C. D., Horn, G., and Horrig, H. B., US Patent, US5600030, 1997 (HOECHST AKTIENGESELLSCHAFT).